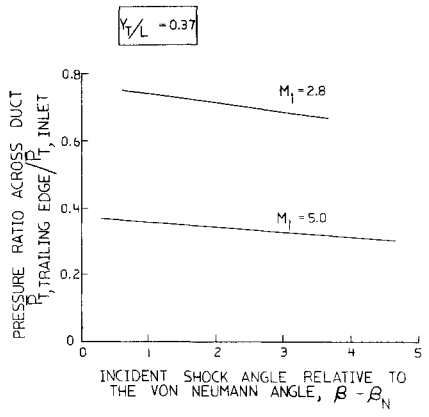

Fig. 4 Mass-averaged stagnation-pressure ratios developed from the predictions in Fig. 3.

of the duct flow is processed by oblique shocks, whereas the remainder encounters a normal shock wave.

One of the advantages of estimating the stagnation pressure losses due only to the flow across shocks is that experimental measurements of the overall P_t drop (which normally include viscous and inviscid contributions) can be better understood. This may help in the design of inlets of hypersonic flow situations where the source of the viscous contribution is difficult to evaluate. (Of course, the shock exists due to the action of viscous forces, but for our purposes the stagnation pressure drop across the shocks can be considered as an inviscid contribution to the overall stagnation loss in the duct.) In addition, if the shock-related contribution turns out to be much larger than that attributable to viscous effects, the designer could introduce methods for minimizing the scale of the shock system (in particular the size of the normal shock) since the largest P_t drops occur there.

As an example, Fig. 3 illustrates the predicted stem heights for freestream Mach numbers of 2.8 and 5.0, and comparison is made with certain unpublished data of Hornung and Robinson.[12] Figure 4 is a graph of the resultant P_t ratio across the duct as a function of the shock-angle difference $\beta - \beta_N$.

The wedge angles corresponding to the incident shock angles shown in Fig. 3 may be rather large for practical hypersonic diffusers. However, the angles shown may be approached during vehicle maneuvering or other transients, and thus the estimates described here may then apply.

Acknowledgments

This work was supported by the NASA Office of Aeronautics and Space Technology under the Hypersonic Training and Research Program, Grant NAGW 966.

References

[1]Goldberg, T. J., and Hefner J. N., "Starting Phenomena for Hypersonic Inlets with Thick Turbulent Boundary Layers at Mach 6," NASA TN D-6180, 1971.

[2]Zucrow, M. J., and Hoffmann, J. D., *Gas Dynamics,* Vol. 1, Wiley, New York, 1976.

[3]Henderson, L. F., and Lozzi, A., "Further Experiments on Transition to Mach Reflexion," *Journal of Fluid Mechanics,* Vol. 94, Pt. 3, 1979, pp. 541-559.

[4]von Neumann, J., "Oblique Reflection of Shocks," Navy Department (Bureau of Ordnance), Washington, DC, *Explosives Research Rept.* No. 12, 1943; see also *Collected Works,* Vol. 6, Pergamon, Oxford, 1963, pp. 238-299.

[5]Hornung, H. G., and Robinson, M. L., "Transition from Regular to Mach Reflection of Shock Waves, Part 2: The Steady-Flow Criterion," *Journal of Fluid Mechanics,* Vol. 123, 1982, pp. 155-164.

[6]Azevedo, D. J., "Prediction of Length Scales in a Mach Reflection Flowfield," Ph.D. Thesis, SUNY, Dept. of Mechanical and Aerospace Engineering, Univ. at Buffalo, May 1989.

[7]Henderson, L. F., "On the Confluence of Three Shock Waves in a Perfect Gas," *The Aeronautical Quarterly,* Vol. XV, May 1964, pp. 181-197.

[8]Hornung, H. G., "Regular and Mach Reflection of Shock Waves," *Annual Review of Fluid Mechanics,* Vol. 18, 1987, pp. 33-58.

[9]Ben-Dor, G., "A Reconsideration of the Three-Shock Theory for a Pseudo-Steady Mach Reflection," *Journal of Fluid Mechanics,* Vol. 181, 1987, pp. 467-484.

[10]Back, L. H., and Cuffel, R. F., "Viscous Slipstream Flow Downstream of a Centerline Mach Reflection," *AIAA Journal,* Vol. 9, No. 10, 1971, pp. 2107-2109.

[11]Chow, W. L., and Addy, A. L., "Interaction Between Primary and Secondary Streams of Supersonic Ejector Systems and Their Performance Characteristics," *AIAA Journal,* Vol. 2, No. 4, 1964, pp. 686-695.

[12]Hornung, H. G., personal communication, Graduate Aeronautics Laboratories, California Institute of Technology, 1988.

[13]Courant, R., and Friedrichs, K. O., *Supersonic Flow and Shock Waves,* Vol. 21, *Applied Mathematical Sciences Series,* Springer-Verlag, New York, pp. 340-341.

Transonic Computations on a Natural Grid

R. K. Naeem* and R. M. Barron†
University of Windsor, Windsor, Ontario, Canada

Introduction

IN an earlier paper,[1] the authors have shown that the von Mises transformation provides a convenient computational domain for the finite difference solution of transonic full-potential flows. The resulting natural grid system consists of the streamlines $\Psi = \text{const}$ and the Cartesian coordinate lines $x = \text{const}$, where $\Psi(x,y)$ is the stream function. In this (x,Ψ) system, the computational domain is rectangular, and the coordinate curves $\Psi = \text{const}$ are "body-fitting," thus eliminating the need to develop a body-conforming grid system using numerical grid generation techniques. It can be shown that transonic full-potential flow is governed by[1]

$$y_\Psi^2 y_{xx} - 2y_x y_\Psi y_{x\Psi} + (1 + y_x^2) y_{\Psi\Psi} = \frac{y_x y_\Psi^2 \rho_x}{\rho} - \frac{y_\Psi (1 + y_x^2)\rho_\Psi}{\rho} \tag{1}$$

$$\rho = \left[1 - \frac{(\gamma - 1)M_\infty^2}{2} \left(\frac{1 + y_x^2}{\rho^2 y_\Psi^2} - 1 \right) \right] \frac{1}{\gamma - 1} \tag{2}$$

where $y = y(x,\Psi)$ is the equation defining the von Mises transformation and ρ is the density. Equation (1) may be viewed as a grid generation equation, but actually it represents the physical condition of irrotationality. This equation is solved for the geometrical unknown $y(x,\Psi)$, and hence we may consider Eq.(1) as tieing together the flow geometry and the flow physics. The pressure coefficient is related to ρ by

$$C_p = \frac{2(\rho^\gamma - 1)}{\gamma M_\infty^2} \tag{3}$$

Received May 8, 1989; revision received Nov. 9, 1989.

*Graduate Student, Department of Mathematics and Statistics.

†Professor, Department of Mathematics and Statistics; Director, Fluid Dynamics Research Institute.

Equations (1) and (2) have been solved in Ref. 1 using the artificial density method developed by Hafez et al.[2] Excellent results have been obtained, for both subcritical and supercritical flows, on relatively coarse grids. As the grid is refined, various parameters involved in the artificial density method must be adjusted to achieve convergence. For a NACA 0012 airfoil at $M_\infty = 0.8$, the finest grid for which convergence can be obtained provides approximately 30 surface grid points. Problems occur in the calculation near the airfoil surface in the supersonic region.

Reformulation

In this Note, we present a simple scheme to overcome the aforementioned grid refinement problem. First, one can easily show that the differential operator on the left-hand side of Eq. (1) is always elliptic, even for mixed flows. This appears to be the main source of difficulty when the grid is refined. In view of this, the terms on the right-hand side of Eq. (1) should be incorporated into the differential operator. This can be done by evaluating ρ_x and ρ_Ψ from Eq. (2), substituting into Eq. (1) and rearranging to give[3]

$$\left(y_\Psi^2 - \frac{M_\infty^2}{\rho^{\gamma+1}}\right) y_{xx} - 2y_x y_\Psi y_{x\Psi} + (1+y_x^2) y_{\Psi\Psi} = 0 \qquad (4)$$

This equation is mixed type, elliptic in subsonic regions, and hyperbolic in supersonic regions.

In von Mises coordinates, the boundary conditions associated with flow past a symmetric airfoil $y = f(x)$, $0 \le x \le 1$, at zero angle of attack are Dirichlet type and are given by $y = \Psi$, $\rho = 1$ at infinity and, on $\Psi = 0$,

$$y = \begin{cases} f(x) & \text{if } 0 \le x \le 1 \\ 0 & \text{if } -0 \le x \le 0 \quad \text{or } 1 \le x < \infty \end{cases} \qquad (5)$$

Equations (2) and (4) can be solved using the type dependent differencing scheme proposed by Murman and Cole.[4] Other schemes, such as artificial viscosity or density, can also be used.

Results and Discussion

Calculations based on Eq. (4) were performed for a variety of airfoils, and results are presented for a NACA 0012 airfoil at $M_\infty = 0.63$ and 0.8 in Figs. 1 and 2. All results have been obtained on a clustered grid as in Ref. 1, yielding 60–70 grid points on the airfoil upper surface.

For the subcritical flow illustrated in Fig. 1, the present method, Garabedian and Korn's method,[5] and Sinclair's field panel method[6] give essentially identical results. An example of a supercritical flow is shown in Fig. 2, comparing our results with solutions obtained by Garabedian and Korn and by Sinclair, which are also based on nonconservative formulations, and the results of Jameson and Yoon,[7] obtained from FLO66A code, based on solution of the conservative Euler equations by a multigrid method. Our method, even though nonconservative, accurately predicts both the shock location and strength, perfoming better than Sinclair's method in the shock region and better than the methods of Sinclair and Garabedian and Korn aft of the shock.

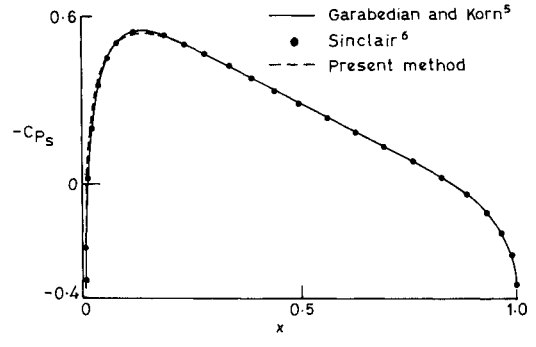

Fig. 1 Surface pressure coefficient, NACA 0012, $M_\infty = 0.63$.

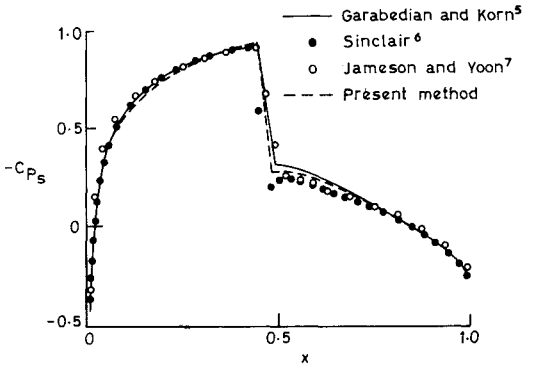

Fig. 2 Surface pressure coefficient, NACA 0012, $M_\infty = 0.8$.

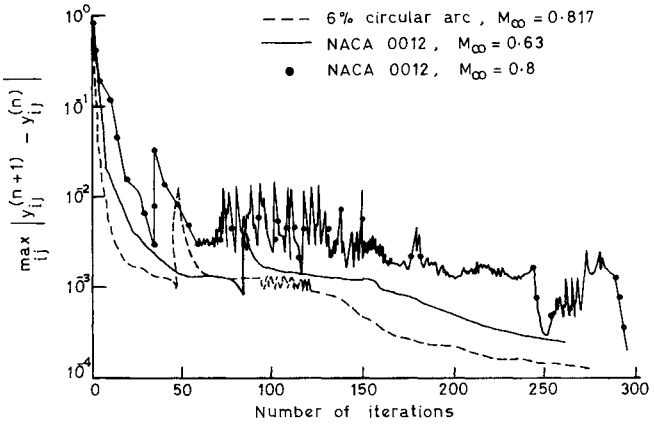

Fig. 3 Convergence history for y.

As is well known, conservative schemes guarantee shock waves in which mass is conserved, but not momentum, while nonconservative schemes do not conserve either mass or momentum. Many researchers therefore believe that conservative schemes are necessary to capture shocks accurately. Others, on the other hand, believe it is better to use a nonconservative scheme that allows for some mass production, thereby providing a more accurate model of a shock wave as an isentropic jump. While not restricting ourselves to either school of thought, we point out that even though our formulation is nonconservative, it does guarantee mass conservation, even across shock waves, by introducing the stream function. Furthermore, our Eq. (4) is actually an equation that generates the grid (streamlines) rather than providing a physical quantity like the velocity potential. An attractive feature of the von Mises formulation is that the equation that generates the grid is obtained from the flow equations and hence provides a natural grid for computation of the flowfield.

The convergence history for y is presented in Fig. 3. A straightforward line relaxation scheme was used, and the error damps out fairly rapidly for subcritical flows. As is expected, convergence is more difficult to achieve for supercritical flow. A strategy similar to that employed by Wigton[8] has been used to prevent any drastic changes between iterations in the density in the supersonic region. Furthermore, we also note that slight variations in density produce relativley large variations in y so that the error in y oscillates considerably before finally dropping to 10^{-4} at about 300 iterations. Undoubtedly, convergence can be improved by employing an acceleration scheme such as Generalized Minimal Residual.[8]

Calculations using the von Mises formulation for nonsymmetric airfoils and nonzero angles of attack have recently been carried out using Eq. (1) rather than Eq. (4). Again, coarse grid solutions show good agreement with the results of other researchers, but fine grid calculations fail to converge.[3] These

calculations are currently being repeated using Eq. (4), and it is expected that accurate fine grid solutions can be achieved.

Acknowledgment

This work was supported by a grant to the second author from the Natural Sciences and Engineering Research Council of Canada. The authors wish to thank J. B. Malone for his comments, which have improved the discussion contained herein, and Denis Jones from the National Aeronautical Establishment for his valuable suggestions, which have contributed to the success of this formulation.

References

[1]Barron, R. M., and Naeem, R. K., "Numerical Solution of Transonic Flows on a Streamfunction Co-ordinate System," *International Journal for Numerical Methods in Fluids,* Vol. 9, No. 10, 1989, pp. 1183-1193.

[2]Hafez, M., Murman, E. M., and South, J., "Artificial Compressibility Methods for Numerical Solution of the Transonic Full Potential Equation," AIAA Paper 78-1148, July 1978.

[3]Naeem, R. K., "Computation of Transonic Flows Using a Streamfunction Coordinate System," Ph.D. Dissertation, University of Windsor, Windsor, Ontario, Canada, 1988.

[4]Murman, E. M., and Cole, J. D., "Calculation of Plane Steady Transonic Flows," *AIAA Journal,* Vol. 9, No. 1, 1971, pp. 114-121.

[5]Garabedian, P. R., and Korn, D., "Analysis of Transonic Airfoils," *Communications of Pure and Applied Mathematics,* Vol. 24, 1971, pp. 841-851.

[6]Sinclair, P. M., "An Exact Integral (Field Panel) Method for the Calculation of Two Dimensional Transonic Potential Flow around Complex Configurations," *Aeronautical Journal,* Vol. 25, No. 896, 1986, pp. 227-236.

[7]Jameson, A., and Yoon, S., "Lower-Upper Implicit Schemes with Multiple Grids for the Euler Equations," *AIAA Journal,* Vol. 25, No. 7, 1987, pp. 929-935.

[8]Wigton, L. B., "Application of MACSYMA and Sparse Matrix Technology to Multielement Airfoil Calculations," AIAA Paper 87-1142, 1987.

General Purpose Program to Generate Compatibility Matrix for the Integrated Force Method

J. Nagabhusanam*
Indian Institute of Science, Bangalore, India
and
S. N. Patnaik†
NASA Lewis Research Center, Cleveland, Ohio

Introduction

THE novel formulation termed the "integrated force method" (IFM) has been established in recent years for analysis, and design of structures.[1-8] In the integrated force method of analysis, a structure idealized by finite elements is designated as "structure (n,m)" where (n,m) are the force and displacement degrees of freedoms of the discrete model, respectively. The structure (n,m) has m equilibrium equations and $r=(n-m)$ compatibility conditions. The generation of the equilibrium equation is straightforward. The generation of the compatibility condition is intricate. We have introduced the concepts to generate compatibility conditions in Refs. 5 and 6. The earlier work was confined to 1) field compatibility conditions only and 2) structure types considered were limited to frame works and plates but not their combinations. The distinct features of this Note from earlier publications are 1) both field and boundary compatibility conditions are examined, 2) different element types are used in the finite element idealization, and 3) a key feature termed "node determinancy" has been introduced. The node determinancy concept enables elimination of nodes of a discrete model at the intermediate stage of the generation of compatibility conditions, which in turn reduces the complexity of the deformation displacement relations. This process enhances computational efficiency.

The two key equations of IFM are Eq. (1) calculation of forces, and Eqs. (2), calculation of displacements of a structure (n,m)[1,3]:

$$\begin{bmatrix} [B] \\ [C][G] \end{bmatrix} F = \begin{Bmatrix} P \\ \hline \delta R \end{Bmatrix} \quad \text{or,} \quad [S]\{F\} = \{P\}^* \tag{1}$$

where $[B]$ is the $(m\times n)$ equilibrium matrix, $[C]$ the $(r\times n)$ compatibility matrix, $[G]$ the $(n\times n)$ concatenated flexibility matrix, $\{P\}$ the m-component load vector, $\{\delta R\}$ the r-component effective initial deformation vector, $\{\delta R\} = -[C]\{\beta_0\}$, where, $\{\beta_0\}$ is the n-component initial deformation vector, and $[S]$ the $(n\times n)$ governing matrix.

Displacements $\{X\}$ are obtained from the forces $\{F\}$ by back substitution:[3]

$$\{X\} = [J]\{[G]\{F\} + [\beta_0]\} \tag{2a}$$

where $[J]$ is the $(m\times n)$ deformation coefficient matrix defined as

$$[J] = m \text{ rows of } [[S]^{-1}]^T \tag{2b}$$

In this Note, the generation of the compatibility matrix $[C]$ is presented in brief.

Strain Formulation of St. Venant

The strain formulation of St. Venant is illustrated taking the example of a plane stress elasticity problem. The strain displacement relations of the problem can be written as

$$\epsilon_x = \frac{\partial u}{\partial x}, \quad \epsilon_y = \frac{\partial v}{\partial y}, \quad \gamma_{xy} = \frac{\partial u}{\partial y} + \frac{\partial v}{\partial x} \tag{3}$$

In Eq. (3), three strain components (ϵ_x, ϵ_y, and γ_{xy}) are expressed in terms of two displacements (u, v).Thus, there is a constraint on strains, which is obtained by the elimination of the displacements. This constraint is the compatibility condition, which has the following form:

$$\frac{\partial^2 \epsilon_x}{\partial y^2} + \frac{\partial^2 \epsilon_y}{\partial x^2} - \frac{\partial^2 \gamma_{xy}}{\partial x \partial y} = 0 \tag{4}$$

The two steps of strain formulation of elasticity are as follows:

Step 1. Establish the strain displacement relations [Eq. (3)].

Step 2. Eliminate displacements from Eq. (3) to obtain the compatibility condition, Eq. (4).

Compatibility Conditions of Finite Element Analysis

St. Venant's fomulation for elastic continua has been extended to finite element analysis to generate discrete compatibility conditions. In the first step, the deformation displacement relations of a finite element analysis (which are

Received June 6, 1988; revision received May 18, 1989.

*Associate Professor.
†Senior NRC Fellow.